



Versatile surface for solid–solid/liquid–solid triboelectric nanogenerator based on fluorocarbon liquid infused surfaces

Jihoon Chung, Handong Cho, Hyungseok Yong, Deokjae Heo, You Seung Rim & Sangmin Lee

To cite this article: Jihoon Chung, Handong Cho, Hyungseok Yong, Deokjae Heo, You Seung Rim & Sangmin Lee (2020) Versatile surface for solid–solid/liquid–solid triboelectric nanogenerator based on fluorocarbon liquid infused surfaces, *Science and Technology of Advanced Materials*, 21:1, 139–146, DOI: [10.1080/14686996.2020.1733920](https://doi.org/10.1080/14686996.2020.1733920)

To link to this article: <https://doi.org/10.1080/14686996.2020.1733920>



© 2020 The Author(s). Published by National Institute for Materials Science in partnership with Taylor & Francis Group.



Accepted author version posted online: 25 Feb 2020.
Published online: 05 Mar 2020.



Submit your article to this journal [↗](#)



Article views: 303



View related articles [↗](#)



View Crossmark data [↗](#)

Versatile surface for solid–solid/liquid–solid triboelectric nanogenerator based on fluorocarbon liquid infused surfaces

Jihoon Chung^{a*}, Handong Cho^{b*}, Hyungseok Yong^a, Deokjae Heo^a, You Seung Rim^c and Sangmin Lee^a

^aSchool of Mechanical Engineering, Chung-ang University, Seoul, Republic of Korea;

^bDepartment of Mechanical Engineering, Mokpo National University, Jeollanam-do, Republic of Korea;

^cSchool of Intelligent Mechatronics Engineering, Sejong University, Seoul, Republic of Korea

ABSTRACT

The triboelectric nanogenerator (TENG) is a recent mechanical energy harvesting technology that has been attracting significant attention. Its working principle involves the combination of triboelectrification and electrostatic induction. The TENG can harvest electrical energy from both solid–solid and liquid–solid contact TENGs. Due to their physical difference, triboelectric materials in the solid–solid TENG need to have high mechanical properties and the surface of the liquid–solid contact TENG should repel water. Therefore, the surface of the TENG must be versatile for applications in both solid–solid and liquid–solid contact environments. In this work, we develop a solid–solid/liquid–solid convertible TENG that has a slippery liquid-infused porous surface (SLIPS) at the top of the electrode. The SLIPS consists of a HDFS coated hierarchical $\text{Al}(\text{OH})_3$ structure and fluorocarbon liquid. The convertible TENG developed in this study is capable of harvesting electricity from both solid–solid and liquid–solid contacts due to the high mechanical property of $\text{Al}(\text{OH})_3$ and the water-based liquid repelling nature of the SLIPS. When the contact occurs in freestanding mode, electrical output was generated through solid–solid/liquid–solid sliding motions. The convertible TENG can harvest electricity from both solid–solid and liquid–solid contacts; thus, it can be a unified solution for TENG surface fabrication.

ARTICLE HISTORY

Received 24 October 2019

Revised 20 February 2020

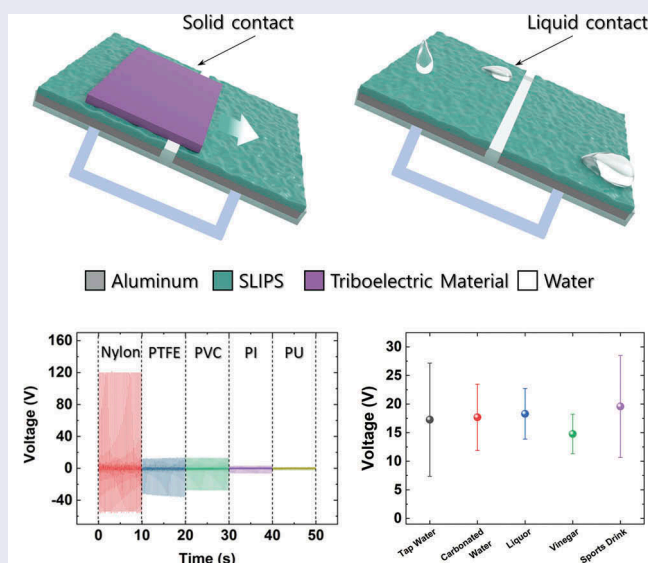
Accepted 20 February 2020

KEYWORDS

Triboelectric nanogenerator; energy harvesting; versatile surface; slips; hierarchical structure

CLASSIFICATION

206 Energy conversion / transport / storage / recovery; 212 Surface and interfaces



1. Introduction

Owing to the rising demand for portable electronics, an increasing number of studies have focused on harvesting electrical energy from ambient sources, including solar [1–3], thermal [4–6], and salinity difference [7–9]. Among these, mechanical energy

sources are suitable for harvesting electrical energy since they are less affected by external conditions, such as weather, temperature, and location. Several technologies have been developed for the effective conversion of mechanical energy into electricity, including piezoelectric transducers [10–12], and

CONTACT You Seung Rim  youseung@sejong.ac.kr  School of Intelligent Mechatronics Engineering, Sejong University, 209, Neungdong-ro, Gwangjin-gu, Seoul, Republic of Korea; Sangmin Lee  slee98@cau.ac.kr  School of Mechanical Engineering, Chung-ang University, 84, Heukseok-ro, Dongjak-gu, Seoul, Republic of Korea

*These authors contributed equally in this work.

© 2020 The Author(s). Published by National Institute for Materials Science in partnership with Taylor & Francis Group.

This is an Open Access article distributed under the terms of the Creative Commons Attribution License (<http://creativecommons.org/licenses/by/4.0/>), which permits unrestricted use, distribution, and reproduction in any medium, provided the original work is properly cited.

electromagnetic induction [13–15]. Among these technologies, the triboelectric nanogenerator (TENG), a recently developed mechanical energy harvesting technology, has been attracting significant attention; its working principle is based on the combination of triboelectrification and electrostatic induction [16–19]. In typical TENGs, the electrode is covered with a polymer material to maximize the surface charge, after which it is placed in contact–separation with a counter-charged triboelectric material to generate electricity [20–23]. This counter-charged triboelectric material can be either solid or liquid depending on the working condition [24–27]. Both solid–solid and liquid–solid contact TENGs have distinct characteristics due to their different physical phases. Due to this difference, these two TENGs require different material properties; triboelectric materials in solid–solid TENGs require high mechanical properties for a long lifespan, and the surface of liquid–solid contact TENGs needs to be water repellent for constant liquid separation [28–31]. Previous studies have presented these TENGs as separate devices; therefore, the triboelectric surfaces of TENGs were developed separately as well. However, for a TENG to harvest electricity from ambient mechanical energy sources such as wind and raindrops, it must be able to adapt to both solid–solid and liquid–solid contact environments. Therefore, a unified TENG surface that is capable of effectively harvesting electrical energy from both solid–solid and liquid–solid contacts is required.

In this study, we develop a solid–solid/liquid–solid convertible TENG that has a slippery liquid-infused porous surface (SLIPS) at the top of its electrode. On this device, a low-surface tension fluorocarbon liquid (perfluoropolyether, PFPE, Krytox) was placed over a trichloro(1H,1H,2H,2H-perfluorooctyl) silane (HDFS)-coated $\text{Al}(\text{OH})_3$ micro-/nanostructure on the aluminum surface. Due to the large number of fluorine atoms on the surface, both the PFPE liquid and HDFS-coated surface can be negatively charged during the contact–separation process, which can lead to the generation of electrical energy from the solid–solid contact. In addition, the surface can effectively repel water-based liquids; thus, it can induce constant contact and separation between the liquid and the TENG surface. The convertible TENG developed in this study could generate electrical energy when in contact with various water-based liquids, such as tap water, carbonated water, liquor, vinegar, and sports drink. When the contact occurred in the freestanding mode, electrical energy was generated from the solid–solid and liquid–solid sliding motions. Thus, this paper presents a unified TENG surface that can effectively harvest electrical energy from both solid–solid and liquid–solid mechanical input.

2. Materials and Methods

2.1 The fabrication of HDFS coated $\text{Al}(\text{OH})_3$ surface with PFPE liquid

First, a 1 mm-thick bare aluminum plate was cleaned with deionized water and ethyl alcohol and dried after rinsing. Thereafter, the aluminum plate was dipped into a 0.5 M NaOH (98%, Samchun Chemical, Korea) solution for 1 min and, subsequently, in boiling water for 10 min. To fabricate a hierarchical structure, the aluminum substrate was etched in a 1 M HCl (35–37%, Samchun Chemical, Korea) solution at 80°C for 2 min. The fabricated surface was rinsed with deionized water again and dried at 60°C for 24 h. For the HDFS coating, the aluminum substrate with a hierarchical structure was immersed in a 0.1 v/v% hexane (96%, Samchun Chemical, Korea) solution of HDFS (Gelest, USA) for 10 min at room temperature. Subsequently, the treated sample was thoroughly rinsed with n-hexane and, thereafter, dried at 110°C for 10 min. PFPE liquid was applied on the fabricated aluminum surface and spin-coated at 500 rpm for 1 min. The final fabricated surface was wired and attached to the acrylic substrate for electrical measurement.

2.2 Measurements

The electrical measurements including voltage and current measurements were conducted using a mixed domain oscilloscope (MDO 3014, Tektronix Co.) and a low-noise current preamplifier (SR570, Stanford Research Systems Co.). The vertical mechanical input was provided by a vibration tester (ET-126B-4, Labworks Co.) connected to an amplifier (pa-151, Labworks Co.) and function generator (AFG3012C, Tektronix Co.).

2.3 Liquid materials

The liquids used in this study are tap water, carbonated water, liquor (Chamisul, 17.8% alcohol, HITEJINRO Co.), vinegar (Apple vinegar, Ottogi Co.), and sports drink (Pocari Sweat, Donga-Otsuka Co.).

3. Results and Discussion

Figure 1 shows the schematic illustration and magnified images of the micro-/nanostructures on the aluminum surface. As shown in Figure 1(a), the hierarchical structure of $\text{Al}(\text{OH})_3$ is constructed on the aluminum surface. On the outer side of the $\text{Al}(\text{OH})_3$ layer, a self-assembled monolayer coating of HDFS is fabricated. The PFPE liquid is applied to the hydrophobic hierarchical structure to form a SLIPS. The SLIPS is extremely liquid-repellent, and it can effectively repel water-based liquids [32]. In this study, 1 mL of liquid PFPE is applied to the hierarchical structure and spin-coated for 1 min at

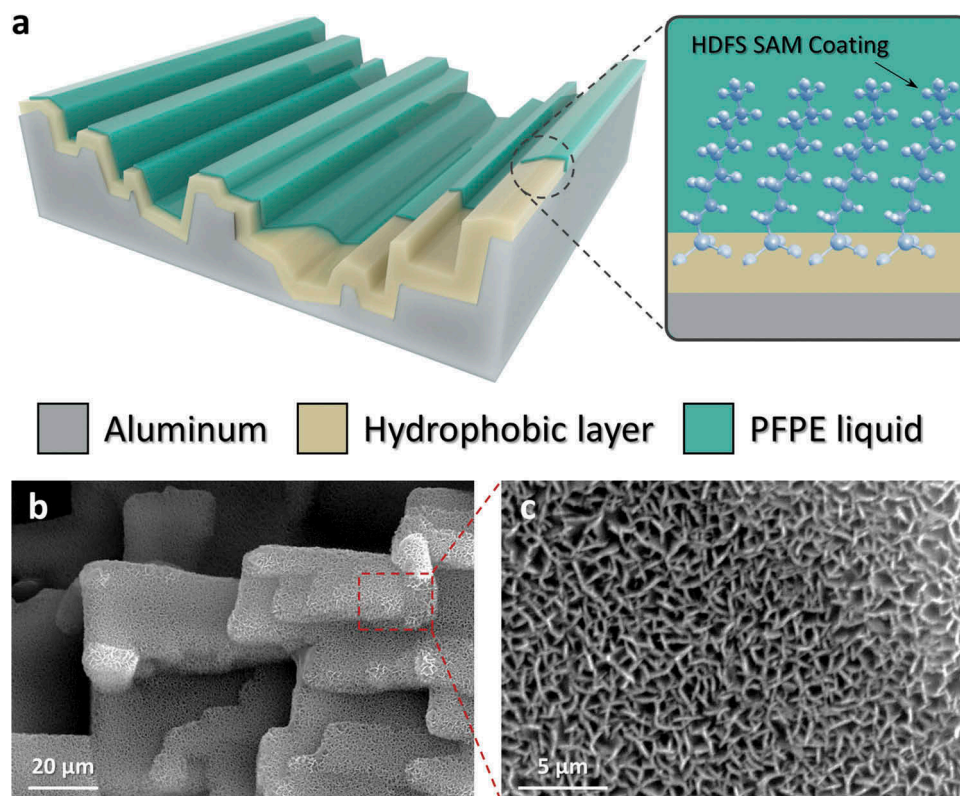


Figure 1. (a) Schematic illustration of the solid–solid/liquid–solid convertible TENG. SAM stands for self-assembled monolayer. Field emission scanning electron microscopy (FE-SEM) image of the (b) microstructures and (c) nanostructures on the aluminum surface.

500 rpm to form an evenly distributed thin liquid layer. Figures 1(b,c) and S1 are the magnified images of the hierarchical structure taken by FE-SEM. As shown in the image, both a micro-sized stair-like structure (Figure 1(b)) and a nano-sized wall structure (Figure 1(c)) are formed on the aluminum surface.

In TENGs, selecting a material with a high surface charge is important. A high surface charge will facilitate the flow of electrons, which would, in turn, generate a relatively high electrical output. Generally, materials with a high electron affinity have a corresponding high surface charge. This accounts for the high usage frequency of fluoropolymers, such as polytetrafluoroethylene (PTFE), in TENGs. For comparison with the material used in this device, the PFPE liquid can be expressed as $F-(CF(CF_3)-CF_2-O)_n-CF_2CF_3$, where n lies within the range of 10–60, and HDFs can be expressed as $CF_3(CF_2)_5CH_2CH_2SiCl_3$. Both the PFPE liquid and HDFs contain a large number of fluorine atoms that has a high electron affinity. Therefore, the PFPE liquid-applied HDFs surface, which has a high negative surface charge, can be suitable for the solid–solid contact. In addition, the hierarchical structure on top of aluminum is that of $Al(OH)_3$, which has more mechanical properties than PTFE [33,34]. The TENG generates electrical output through mechanical contact and friction; consequently, a long lifespan can be expected with high mechanical properties.

Figure 2(a) is a schematic illustration of the solid–solid contact TENG working principle, which is the same as that of the single electrode TENG [35,36]. As shown in the figure, the triboelectric material at the top is positively charged and the PFPE liquid-applied HDFs surface is negatively charged due to repeated contact and separation processes. The aluminum electrode at the bottom is affected by the electric field of the SLIPS. As external pressure is applied to the triboelectric material, its surface approaches the single electrode TENG surface. The electrical equilibrium of the aluminum electrode is disrupted by the electric field on the surface of the triboelectric material, and electrons flow into the aluminum electrode. When the triboelectric material contacts the SLIPS, the aluminum electrode attains electrical equilibrium once more. Once the external pressure is eliminated, the triboelectric material detaches from the SLIPS and electrons flow back to the electrical ground owing to the electric field of the SLIPS. By repeating this process, the TENG can produce alternating current (AC) by the contact–separation process between two solid materials.

Figure 2(b,c) show the open-circuit voltage (V_{OC}) and closed-circuit current (I_{CC}) outputs of the device, respectively. The TENG was supplied with 6 Hz input using a mechanical vibration tester. As shown in the plot, the TENG generated the highest output when nylon came in contact with the SLIPS. The nylon

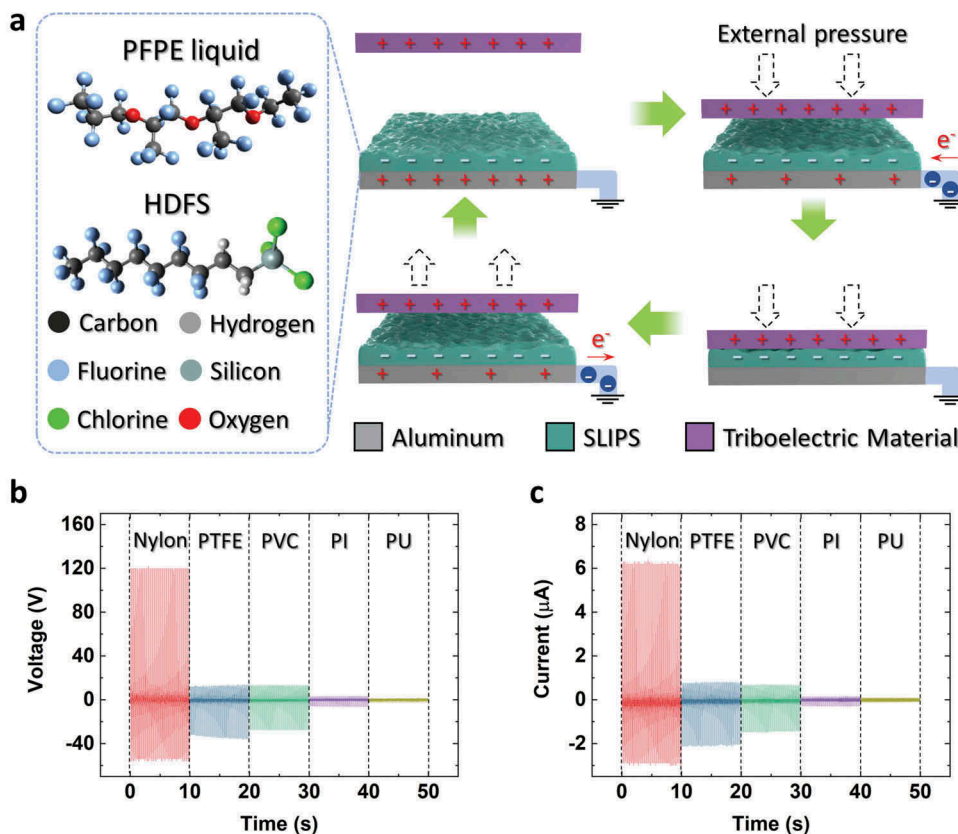


Figure 2. (a) Schematic illustration and working mechanism of the solid–solid contact TENG. (b) V_{OC} and (c) I_{CC} outputs of the convertible TENG depending on various materials. PVC, PI and PU stand for polyvinyl chloride, polyimide, and polyurethane, respectively.

contact produced high positive peaks, while the PTFE and PVC contacts produced high negative peaks. This is because the PTFE and PVC surfaces became negatively charged when they came in contact with the SLIPS, whereas the nylon surface became positively charged. The SLIPS was formed with the PFPE liquid and HDFS, and for it to produce the highest output when in contact with nylon, it should be negatively charged. When the contact material is nylon, the TENG produces a maximum V_{OC} of 122 V and a maximum I_{CC} of 6.4 μA .

The TENG can generate electrical energy from liquid–solid contact as well because the SLIPS has an excellent liquid repellent property. Figure 3(a) shows the working mechanism of the liquid–solid contact TENG [37,38]. In Figure 3(a), the waterdrop becomes positively charged when it moves through the air and water pipe, and the SLIPS is negatively charged due to the constant contact and separation of the waterdrop. Due to the negatively charged SLIPS, the aluminum electrode will have a positive net charge. When the waterdrop approaches the SLIPS, the positively-charged waterdrop neutralizes the negatively charged SLIPS; therefore, the electrons will flow from the electrical ground to the aluminum electrode. After the waterdrop attaches completely, there will be a minimal surface area difference as the waterdrop moves toward the edge of the TENG. When the

waterdrop separates from the TENG, the electrons will flow back to the ground. A repetition of the waterdrop contact and separation processes produces AC.

In a typical TENG, a thin layer of dielectric material is preferred to effectively induce charges on the electrode [39,40]. In this device, the thickness of the dielectric material is equal to the amount of the PFPE liquid remaining on the hierarchical structure. As shown in Figure 3(b–i), the PFPE liquid forms a flat liquid film when initially applied. However, when spin-coated, it forms a thin liquid film along the hierarchical structure on the aluminum electrode (Figure 3(b–ii)). This thickness difference of the PFPE liquid affects the power generation of the device. For comparison, two devices with identical surfaces that have equal amounts of the PFPE liquid were prepared. Subsequently, one sample was spin-coated for 1 min at 500 rpm. Afterward, 2 mL of tap water was dropped on each sample from a height of 20 cm for electrical measurement. As shown in the plot of Figure 3(c), the spin-coated devices produced a peak voltage approximately 5 times higher than that produced by the non-spin-coated device. This indicates that the PFPE liquid is able to properly charge the aluminum electrode when the PFPE liquid film is thin. In addition, the peak-like shape of $\text{Al}(\text{OH})_3$ hierarchical structure accumulates the electrical charge and enhances the output accordingly.

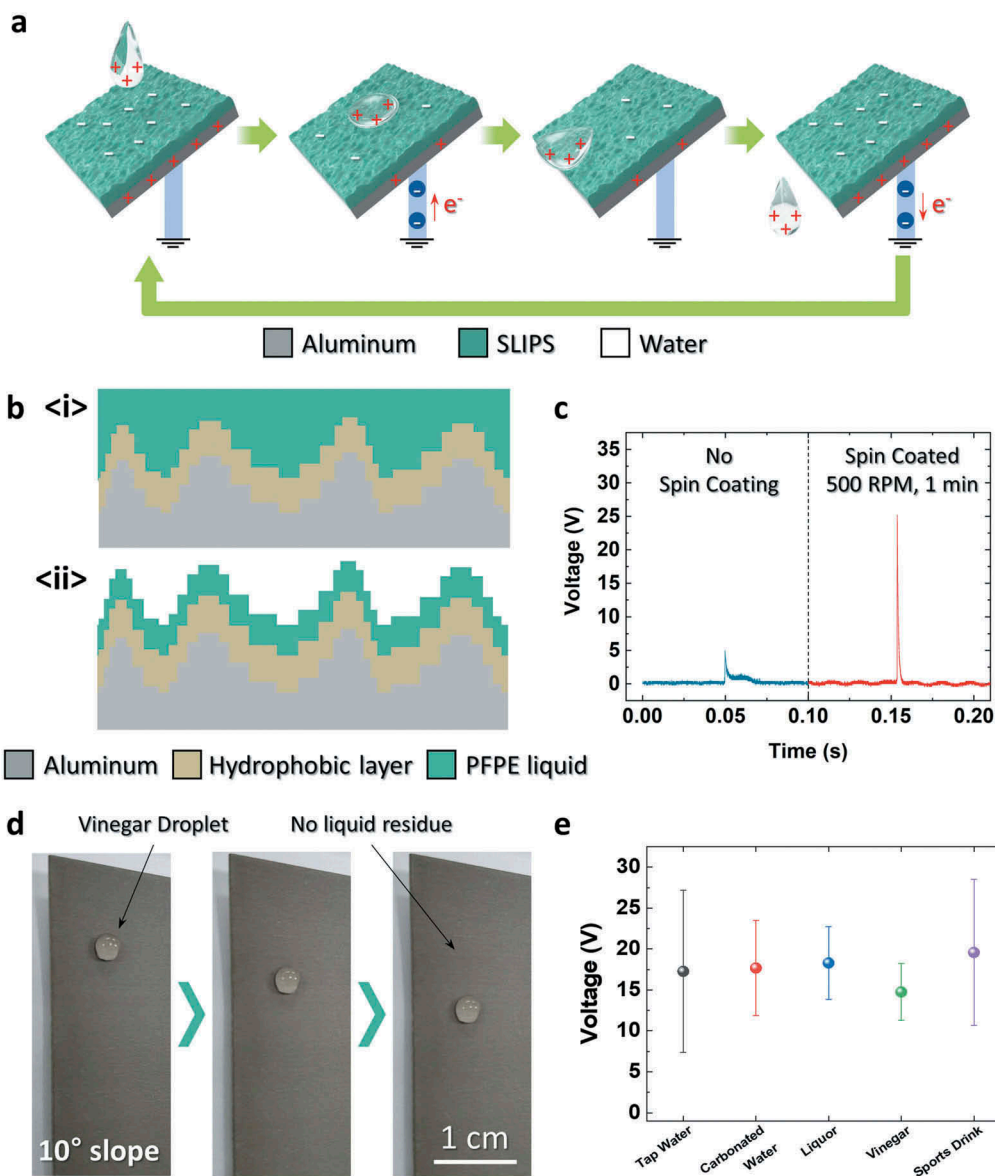


Figure 3. (a) Working mechanism of the liquid–solid contact TENG. (b) Thickness difference of the PFPE liquid depending on the spin-coating process. (c) V_{OC} output depending on the spin-coating process. (d) Photographs of the vinegar droplet on a 10°-slope SLIPS. (e) Average maximum peak voltage of the liquid–solid contact TENG depending on the liquid.

The SLIPS at the top of the aluminum electrode can repel water-based liquids effectively, including various liquids that are frequently used in everyday life. Figures 3(d) and S2 are photographs of 30 μ L-drops of various liquids on a SLIPS, which were taken at 2 s intervals. The surface was tilted 10° for the liquid drop to gravitate toward the edge due to gravitational force. The tested liquids are tap water, carbonated water, liquor (17.8% alcohol), vinegar, and sports drink. As shown in the images, all these liquids slipped to the ground without leaving liquid residues on the surface. Photograph of hierarchical structure without PFPE liquid is shown in Figure S3, after 100 mL of vinegar was poured. As shown in Figure S3, there are many liquid drops pinned on the surface after pouring. These liquid drops left from on the surface would lower the electrical potential difference between liquid and electrode resulting lower output [37]. When

2 mL-liquid drops were dropped from a height of 20 cm, each liquid produced electrical output, as shown in Figure 3(e). The plot represents the maximum peak voltage when each liquid drop was dropped. Although the standard deviations of the voltage peaks are quite large due to the unconstrained nature of the drops, each liquid drop produced 15–20 V on average. This shows the possibility of producing electricity from common used water-based liquids using a SLIPS.

A single-electrode-mode TENG discussed in previous paragraphs required an electrical ground for electrons to flow in between. For portable applications, having extra components, such as an electrical ground, can be a critical factor. Therefore, in Figure 4(a), two aluminum electrodes with SLIPSs were attached to an acrylic substrate to generate electrical output in freestanding mode. In the freestanding mode, the TENG can effectively

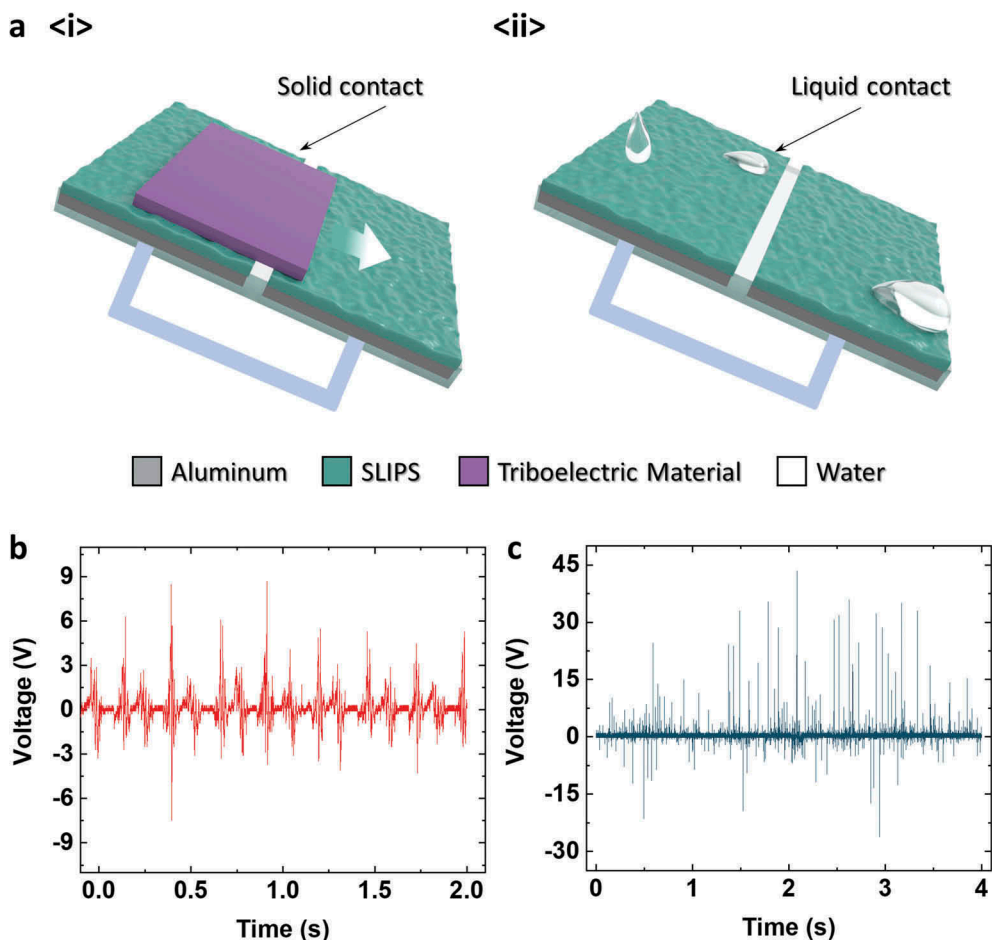


Figure 4. (a) Schematic illustration of the solid–solid/liquid–solid freestanding TENG. V_{OC} output of the convertible TENG from (b) solid–solid sliding and (c) tap water spraying.

convert sliding mechanical input into electricity. Figure 4 (a–i) shows the solid–solid contact freestanding TENG, and Figure 4(a–ii) shows the liquid–solid contact freestanding TENG. For the solid–solid contact TENG, nylon was used as the triboelectric material, and the sliding input was supplied manually (by hand). For the liquid–solid contact TENG, water was sprayed using a commercial shower head. The produced V_{OC} output is shown in Figure 4(b,c), and the current output is shown in Figure S4. As shown in Figures 4(b) and S4 (a), both the V_{OC} and I_{CC} show periodic outputs as the solid triboelectric material slides in between two electrodes. In contrast, Figures 4(c) and S4(b) show rather random peak outputs due to the combination of water-drops falling on to the surface randomly and waterdrops slipping to the ground. The electrical outputs by the solid triboelectric material and liquid drop show their possible application in unified-surface convertible TENGs.

4. Conclusions

In summary, we developed a solid–solid/liquid–solid convertible TENG using a PFPE infused surface. Using fluorine abundant materials, the SLIPS could be charged negatively when it came in contact with a counter-charged triboelectric material and utilized

in both solid–solid and liquid–solid contact environments. Due to the negatively charged surface, the convertible TENG produced the highest peak V_{OC} output of 122 V and peak I_{CC} output of 6.4 μA when the contact material was solid nylon. In addition, the SLIPS on the convertible TENG was capable of repelling water-based liquids. The convertible TENG could produce 15–20 V peak voltages on average using various common used liquids. To demonstrate the applicability of the solid–solid/liquid–solid convertible TENG, a freestanding mode TENG was developed that could harvest electricity from the sliding mechanical motions of both solid and liquid materials. Therefore, the convertible TENG that can harvest electricity from both solid–solid and liquid–solid contacts can be unified solution for TENG surface fabrication.

Disclosure statement

No potential conflict of interest was reported by the authors.

Funding

This research was supported by the Chung-Ang University Research Grants in 2018, and National research Foundation of Korea [NRF-2019R1F1A1061646].

References

- [1] Chai Z, Zhang N, Sun P, et al. Tailorable and wearable textile devices for solar energy harvesting and simultaneous storage. *ACS Nano*. 2016;10(10):9201–9207.
- [2] Li C, Liu Y, Huang X, et al. Direct sun-driven artificial heliotropism for solar energy harvesting based on a photo-thermomechanical liquid-crystal elastomer nanocomposite. *Adv Funct Mater*. 2012;22(24):5166–5174.
- [3] Smith JG, Fauchaux JA, Jain PK. Plasmon resonances for solar energy harvesting: a mechanistic outlook. *Nano Today*. 2015;10(1):67–80.
- [4] Abraham TJ, MacFarlane DR, Pringle JM. High Seebeck coefficient redox ionic liquid electrolytes for thermal energy harvesting. *Energy Environ Sci*. 2013;6(9):2639–2645.
- [5] Han T, Zhao J, Yuan T, et al. Theoretical realization of an ultra-efficient thermal-energy harvesting cell made of natural materials. *Energy Environ Sci*. 2013;6(12):3537–3541.
- [6] Karker N, Dharmalingam G, Carpenter MA. Thermal energy harvesting plasmonic based chemical sensors. *ACS Nano*. 2014;8(10):10953–10962.
- [7] Brogioli D, Zhao R, Biesheuvel P. A prototype cell for extracting energy from a water salinity difference by means of double layer expansion in nanoporous carbon electrodes. *Energy Environ Sci*. 2011;4(3):772–777.
- [8] Kim J, Kim SJ, Kim D-K. Energy harvesting from salinity gradient by reverse electrodialysis with anodic alumina nanopores. *Energy*. 2013;51:413–421.
- [9] Kim T, Logan BE, Gorski CA. High power densities created from salinity differences by combining electrode and Donnan potentials in a concentration flow cell. *Energy Environ Sci*. 2017;10(4):1003–1012.
- [10] Han SA, Kim TH, Kim SK, et al. Point-defect-passivated MoS₂ nanosheet-based high performance piezoelectric nanogenerator. *Adv Mater*. 2018;30(21):1800342.
- [11] Hinchet R, Lee S, Ardila G, et al. Performance optimization of vertical nanowire-based piezoelectric nanogenerators. *Adv Funct Mater*. 2014;24(7):971–977.
- [12] Wang ZL, Song J. Piezoelectric nanogenerators based on zinc oxide nanowire arrays. *Science*. 2006;312(5771):242–246.
- [13] Dai H, Abdelkefi A, Javed U, et al. Modeling and performance of electromagnetic energy harvesting from galloping oscillations. *Smart Mater Struct*. 2015;24(4):045012.
- [14] Saha C, O'donnell T, Wang N, et al. Electromagnetic generator for harvesting energy from human motion. *Sens Actuators A*. 2008;147(1):248–253.
- [15] Wang H, He C, Lv S, et al. A new electromagnetic vibrational energy harvesting device for swaying cables. *Appl Energy*. 2018;228:2448–2461.
- [16] Heo D, Kim T, Yong H, et al. Sustainable oscillating triboelectric nanogenerator as omnidirectional self-powered impact sensor. *Nano Energy*. 2018;50:1–8.
- [17] Niu S, Liu Y, Wang S, et al. Theory of sliding-mode triboelectric nanogenerators. *Adv Mater*. 2013;25(43):6184–6193.
- [18] Niu S, Liu Y, Wang S, et al. Theoretical investigation and structural optimization of single-electrode triboelectric nanogenerators. *Adv Funct Mater*. 2014;24(22):3332–3340.
- [19] Zi Y, Niu S, Wang J, et al. Standards and figure-of-merits for quantifying the performance of triboelectric nanogenerators. *Nat Commun*. 2015;6:8376.
- [20] Chung J, Heo D, Shin G, et al. Ion-enhanced field emission triboelectric nanogenerator. *Advan Energy Mater*. 2019;9(37):1901731.
- [21] Chung J, Yong H, Moon H, et al. Capacitor-integrated triboelectric nanogenerator based on metal-metal contact for current amplification. *Adv Energy Mater*. 2018;8(15):1703024.
- [22] He X, Guo H, Yue X, et al. Improving energy conversion efficiency for triboelectric nanogenerator with capacitor structure by maximizing surface charge density. *Nanoscale*. 2015;7(5):1896–1903.
- [23] Wang S, Xie Y, Niu S, et al. Maximum surface charge density for triboelectric nanogenerators achieved by ionized-air injection: methodology and theoretical understanding. *Adv Mater*. 2014;26(39):6720–6728.
- [24] Kim T, Kim DY, Yun J, et al. Direct-current triboelectric nanogenerator via water electrification and phase control. *Nano Energy*. 2018;52:95–104.
- [25] Li X, Tao J, Wang X, et al. Networks of high performance triboelectric nanogenerators based on liquid-solid interface contact electrification for harvesting low-frequency blue energy. *Adv Energy Mater*. 2018;8(21):1800705.
- [26] Lin ZH, Cheng G, Lin L, et al. Water-solid surface contact electrification and its use for harvesting liquid-wave energy. *Angew Chem*. 2013;52(48):12545–12549.
- [27] Tang W, Jiang T, Fan FR, et al. Liquid-metal electrode for high-performance triboelectric nanogenerator at an instantaneous energy conversion efficiency of 70.6%. *Adv Funct Mater*. 2015;25(24):3718–3725.
- [28] Chung J, Heo D, Kim B, et al. Superhydrophobic water-solid contact triboelectric generator by simple spray-on fabrication method. *Micromachines*. 2018;9(11):593.
- [29] Hou H, Xu Q, Pang Y, et al. Efficient storing energy harvested by triboelectric nanogenerators using a safe and durable all-solid-state sodium-ion battery. *Adv Sci*. 2017;4(8):1700072.
- [30] Lee KY, Chun J, Lee JH, et al. Hydrophobic sponge structure-based triboelectric nanogenerator. *Adv Mater*. 2014;26(29):5037–5042.
- [31] Lin Z-H, Cheng G, Wu W, et al. Dual-mode triboelectric nanogenerator for harvesting water energy and as a self-powered ethanol nanosensor. *ACS Nano*. 2014;8(6):6440–6448.
- [32] Wong T-S, Kang SH, Tang SK, et al. Bioinspired self-repairing slippery surfaces with pressure-stable omniphobicity. *Nature*. 2011;477(7365):443.
- [33] Biswas S, Vijayan K. Friction and wear of PTFE—a review. *Wear*. 1992;158(1–2):193–211.
- [34] Pooley CM, Tabor D. Friction and molecular structure: the behaviour of some thermoplastics. *Proc R Soc Lond A Math Phys Sci*. 1972;329(1578):251–274.
- [35] Chen SW, Cao X, Wang N, et al. An ultrathin flexible single-electrode triboelectric-nanogenerator for mechanical energy harvesting and instantaneous force sensing. *Adv Energy Mater*. 2017;7(1):1601255.

- [36] Yang Y, Zhou YS, Zhang H, et al. A single-electrode based triboelectric nanogenerator as self-powered tracking system. *Adv Mater.* 2013;25(45):6594–6601.
- [37] Cho H, Chung J, Shin G, et al. Toward sustainable output generation of liquid–solid contact triboelectric nanogenerators: the role of hierarchical structures. *Nano Energy.* 2019 Feb;56:56–64.
- [38] Lin ZH, Cheng G, Lee S, et al. Harvesting water drop energy by a sequential contact-electrification and electrostatic-induction process. *Adv Mater.* 2014;26(27):4690–4696.
- [39] Dharmasena RDIG, Jayawardena K, Mills C, et al. Triboelectric nanogenerators: providing a fundamental framework. *Energy Environ Sci.* 2017;10(8):1801–1811.
- [40] Zhu G, Zhou YS, Bai P, et al. A shape-adaptive thin-film-based approach for 50% high-efficiency energy generation through micro-grating sliding electrification. *Adv Mater.* 2014;26(23):3788–3796.